Extremely Small, Wide-band Mobile Phone Antennas by Inductive Chassis Mode Coupling

Werner L. Schroeder, Arturo Acuña Vila and Christian Thome
BenQ Mobile GmbH & Co. OHG, D-47463 Kamp-Lintfort, Germany,
phone +492842951768, werner.schroeder@benq.com

***Abstract*— A novel antenna concept for mobile terminals is presented which achieves large bandwidth at negligible extra volume by means of chassis mode tuning and optimally placed inductive coupling elements. The approach is best suited for folder-type ("clam-shell"), slider-type and similar device form factors featuring two separate but electrically interconnected chassis elements. The proposed antenna's mode of operation is discussed in terms of chassis mode resonances and equivalent circuits. Implementation and bandwidth over volume performance are illustrated by simulation results for a dual-feed penta-band antenna case study. As a practical application of high topical interest, an add-on DVB-H antenna for a folder-type phone with a measured return loss of at least 7 dB over the full UHF bands IV and V at negligible extra volume is reported.**

***Index terms* — Mobile antenna**

I. Introduction

Antenna concepts for mobile terminals have undergone significant change during the last decade. External stub antennas have widely been replaced by internal antennas, mostly based on the PIFA concept. Device miniaturization and the ongoing introduction of additional frequency bands are meanwhile pushing the PIFA concept to its limits. The small volume left for the antenna, in particular the trend to very low profile devices, result in insufficient matching bandwidth. Naturally, this problem is most pronounced at lower frequencies, e.g. in the GSM 450/850/900 bands and the DVB-H band.

Progress has been made in recent years in that an improved understanding of the radiation mechanism of small mobile terminals has come about. [1] has drawn attention to the role of the chassis and clarified that the nominal antenna element is in general, in particular at lower frequencies, operating as a chassis mode coupler rather than as a radiator. The use of a simple capacitive chassis mode coupler instead of a conventional PIFA was suggested. Related design studies were reported e.g. in [2]. Obviously, once the dominant role of the chassis for the radiation properties of electrically small mobile terminals is acknowledged, purposeful chassis design and tuning of chassis modes comes into focus. Analysis in terms of characteristic mode theory [3] was addressed e.g. in [4]–[6]. An application oriented, hands-on method for chassis mode analysis was proposed in [7] and techniques for independently tuning bar-type phone chassis resonances in different bands were presented. Such techniques allow for a significant improvement of bandwidth and reduction of volume over that of conventional PIFAs as illustrated for a dual-feed GSM quad-band antenna on a bar-type chassis in [8].

The present contribution explores, to the authors knowledge for the first time, the use of inductive chassis mode couplers, in particular for folder type, slider type and similar mobile phone form factors in the open state. These form factors are nowadays most popular due to allowance for larger keyboard and display while preserving small in-pocket size. Their advantageous electromagnetic properties suggest the use of dedicated miniature "antennas" for open state operation.

II. Concepts of chassis centric design

The dominant role of the chassis for the radiation properties of electrically small mobile terminals is a simple consequence of the relative size of chassis and internal antennas. Assuming typical dimensions, the Chu-limit on radiation quality factor, Q_{rad}, is e.g. at $900\,\mathrm{MHz}$ by a factor of roughly 8 (4) smaller for an open folder-type chassis (bar-type chassis) than for an internal PIFA itself [9]. Purposeful use of the chassis not only can improve bandwidth, which scales inversely with Q_{rad}, but also radiation efficiency, η_{rad}, according to

$$\eta_{\mathrm{rad}} = Q_{\mathrm{diss}}/(Q_{\mathrm{rad}} + Q_{\mathrm{diss}}) \qquad (1)$$

where Q_{diss} denotes the dissipation quality factor. Chassis centric antenna design is involved with 3 main aspects:

(A) For effective coupling between a small coupling element and a (relatively) large chassis, the latter must be designed to expose resonant modes not to far from the intended bands of operation.
(B) These resonant modes must be selected to give rise to a sizeable radiation vector $\boldsymbol{F}$ (see below).
(C) The type of the coupling element (electric or magnetic) and its location on the chassis must be selected to maximize the reaction between the resonant chassis mode and the field of the coupler.

A further aspect, not addressed in this paper, is near field shaping so as to minimize interaction with the user. It generally amounts to a trade-off between bandwidth and SAR. For investigation of aspects (A)–(C) a coupler ("antenna") independent approach is asked for. The usual input impedance focused design and simulation approach is not apt to investigate chassis mode resonances. By a *resonant chassis mode* we refer to a surface current density distribution on the union of the conductive parts of the device which is equiphase and, once excited and left alone, behaves (assuming perfect conductors) as

$$\boldsymbol{J}_{\mathrm{S}}(\boldsymbol{r}', t) = \boldsymbol{J}_{\mathrm{S},i}(\boldsymbol{r}') \exp\left(\mathrm{j}\,\omega_i t - \omega_i t/(2Q_{\mathrm{rad},i})\right) \qquad (2)$$

where subscript i refers to the i-th mode with resonance frequency ω_i and radiation quality factor $Q_{\mathrm{rad},i}$. The current densities $\boldsymbol{J}_{\mathrm{S},i}$ are the zero eigenvalue solutions of the eigenvalue problem for the characteristic modes on conducting bodies derived in [3]. Unfortunately, the solution of open boundary eigenvalue problems is generally not supported in a useful way in commercial field solvers. From an application point of view, however, the subset of resonant modes which couples to plane waves is of dominant interest. Coupler independent analysis of this subset is possible by using the generally available plane wave excitation feature and then post-processing calculated surface current density $\boldsymbol{J}_{\mathrm{S}}(\boldsymbol{r}')$ to identify chassis mode resonances. A most useful quantity in this context is the *radiation vector*

$$\boldsymbol{F}(\boldsymbol{k}) := \int_{\boldsymbol{r}'\in S} \boldsymbol{J}_{\mathrm{S}}(\boldsymbol{r}')\, \mathrm{e}^{\,\mathrm{j}\,\boldsymbol{k}\boldsymbol{r}'}\, \mathrm{d}S. \tag{3}$$

$\boldsymbol{k}$ denotes the wave vector with orientation towards the observation point and S the surface of the conductive chassis. For an electrically small chassis it is well approximated by its first two moments

$$\boldsymbol{F}_0 := \int_{\boldsymbol{r}'\in S} \boldsymbol{J}_{\mathrm{S}}(\boldsymbol{r}')\, \mathrm{d}S = \mathrm{j}\,\omega\boldsymbol{p}, \tag{4}$$

$$\boldsymbol{F}_1(\boldsymbol{k}) := \mathrm{j} \int_{\boldsymbol{r}'\in S} (\boldsymbol{k}\boldsymbol{r}')\boldsymbol{J}_{\mathrm{S}}(\boldsymbol{r}')\, \mathrm{d}S = \mathrm{j}\,\boldsymbol{m}\times\boldsymbol{k} - \frac{\omega}{2}\mathbf{Q}\boldsymbol{k}. \tag{5}$$

$\boldsymbol{p}$, $\boldsymbol{m}$ and $\mathbf{Q}$ denote the electric and magnetic dipole moment and quadrupole tensor, respectively, of $\boldsymbol{J}_{\mathrm{S}}$. Resonant chassis modes which correspond to one of these moments are identified as maxima of the magnitude of the respective moment, over frequency, under plane wave excitation. Since the far field can be written in terms of the radiation vector as

$$\boldsymbol{H}(\boldsymbol{r}) = -\,\mathrm{j}\,\frac{\mathrm{e}^{-\,\mathrm{j}\,kr}}{4\pi r}\boldsymbol{k}\times\boldsymbol{F}(\boldsymbol{k}),\quad \boldsymbol{E}(\boldsymbol{r}) = \frac{-1}{\omega\epsilon_0}\boldsymbol{k}\times\boldsymbol{H}(\boldsymbol{r}) \tag{6}$$

and hence radiated power density in the $\boldsymbol{k}$ direction as

$$S(\boldsymbol{k}) = \frac{Z_0}{32\pi^2 r^2}\left|\boldsymbol{k}\times\boldsymbol{F}(\boldsymbol{k})\right|^2, \tag{7}$$

the resonant modes thus identified also are good radiators. Resonance frequencies ω_i and the associated $Q_{\mathrm{rad},i}$ are found from, e.g. the $|\boldsymbol{F}_0|$ over ω curve (see Fig. 2), by fitting the generic resonator model

$$|\boldsymbol{F}_0| \approx \frac{A_i}{1+\mathrm{j}\,Q_{\mathrm{rad},i}\left(\frac{\omega}{\omega_i}-\frac{\omega_i}{\omega}\right)}. \tag{8}$$

The software IE3D was used for all simulations below.

III. Folder Type Phone Chassis

Common to folder type, slider type and similar mobile phone form factors is the presence of two major separate chassis elements (e.g. base part and flip part) and a comparatively narrow interconnection, usually a shielded flex-PCB. The first two useful modes on a generic folder type chassis, i.e. the $\lambda/2$ and the $3\lambda/2$ resonance are briefly reviewed. Current densities are depicted in Fig. 1. The magnitude of $\boldsymbol{F}_0$ after (4) and of $\boldsymbol{F}_0' := \boldsymbol{F}_0 - \langle \boldsymbol{J}_{\mathrm{S},1}, \boldsymbol{J}_{\mathrm{S}}\rangle / \left\|\boldsymbol{J}_{\mathrm{S},1}\right\|^2 \boldsymbol{F}_{0,1}$, the component of $\boldsymbol{F}_0$ due to the current density orthogonal to that of the first resonance, $\boldsymbol{J}_{\mathrm{S},1}$, are given in Fig. 2. The first resonance is essentially that of a capacitively and inductively loaded dipole and hence has a somewhat increased radiation quality factor, e.g. $Q_{\mathrm{rad},1} = 4.4$ at $\omega_1 = 680\,\mathrm{MHz}$ in the example as opposed to 2.6 for an equal size plate. A useful range for tuning by design of the interconnection's length and width exists. More interesting options exist for the $3\lambda/2$ resonance. As evident from Fig. 1b, it is possible to absorb the centre half-wavelength into the slots between base and flip part. The current densities on the base and flip parts are then co-oriented and add constructively to $\boldsymbol{F}_0$ whereas the counter-oriented currents in the slot region mostly cancel with respect to radiation. Effective length is thereby increased and the radiation pattern, though flattened, preserves a dipole like shape. The $3\lambda/2$ mode can be used over a very large bandwidth as indicated by the very broad maximum of $\boldsymbol{F}_0'$ in the $1.6\ldots2\,\mathrm{GHz}$ region in Fig. 2. Both, the $\lambda/2$ and the $3\lambda/2$ resonance expose a current density maximum on the interconnection. It is therefore suggestive to place inductive couplers in the hinge region to exploit these modes.

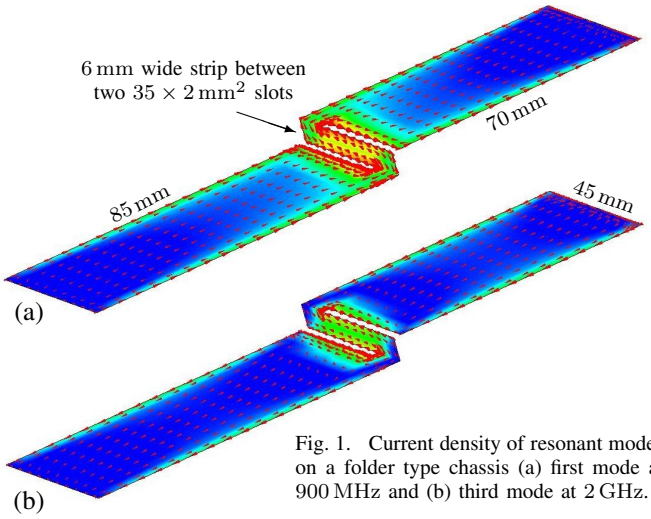

Fig. 1. Current density of resonant modes on a folder type chassis (a) first mode at 900 MHz and (b) third mode at 2 GHz.

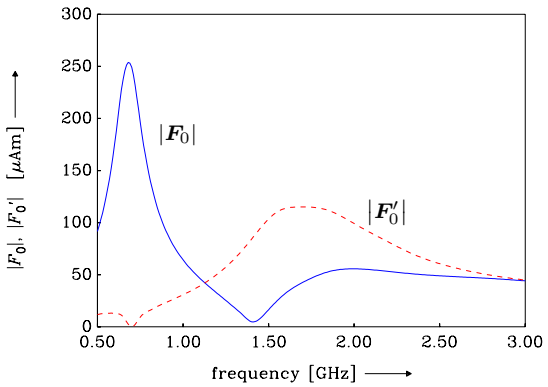

Fig. 2. Magnitude of the first moment of the radiation vector $\boldsymbol{F}_0$ after (4) for the structure of Fig. 1 under broadside, long axis polarized plane wave illumination (solid line). $\boldsymbol{F}_0'$ (dashed line) is due to the current density component $\boldsymbol{J}_{\mathrm{S}}'$ only, defined by $\langle \boldsymbol{J}_{\mathrm{S},1}, \boldsymbol{J}_{\mathrm{S}}'\rangle = 0$.

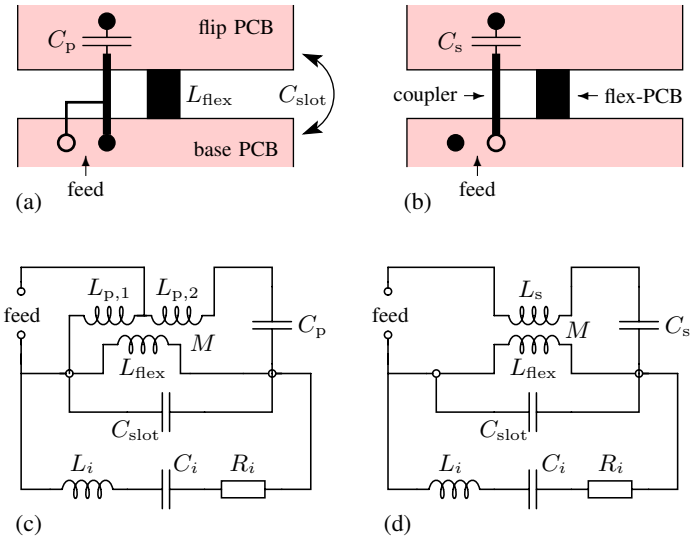

Fig. 3. Schematic construction and qualitative equivalent circuit of inductive couplers on folder type chassis: (a,c) parallel resonant coupler, (b,d) series resonant coupler.

IV. Inductive Couplers

The two basic types of hinge located inductive couplers are schematically shown in Figs. 3a,b. The interconnection between base and flip part is represented by the wide strip. The coupler is simply another line with a series capacitor for resonance tuning. Fig. 3a displays the parallel resonant type, where either end is connected to its respective PCB ground and a tap is foreseen for the feed terminal. The dual, series resonant type, is shown in Fig. 3b. Qualitative equivalent circuits of the chassis – coupler combinations are shown in Fig. 3c,d. L_i, C_i and R_i are introduced to model the i-th chassis mode near resonance without including the additional inductance L_{flex} of the interconnecting strip and the capacitance C_{slot} between base and flip part at the hinge which are separately considered. M denotes the mutual inductance between coupling strip and interconnection. The resonant couplers (at the top of the schematics) are strongly coupled to the chassis mode and thus strongly damped by the radiation resistance R_i of the chassis mode. Despite the miniature size of these "antennas" quality factors are therefore low and large bandwidth can be achieved. Since the electric field strength in the vicinity of such coupler is relatively small, the required keep-out volume around it is also small. Mechanically, a large variety of alternative realizations exists. The couplers can be placed broadside on the interconnection (see Section V) or be placed lateral to the latter (see Section VI), e.g. in form of a separate flexible connection or integrated with the anyway present flex-PCB.

V. Penta-band antenna case study

To illustrate the implementation and performance of inductive couplers the conceptual design of a dual-feed penta-band antenna (GSM850/900, DCS, PCS, UMTS band) on a generously simplified geometry is investigated by simulation (Fig. 4). The interconnection is shaped in principle as in Fig. 1

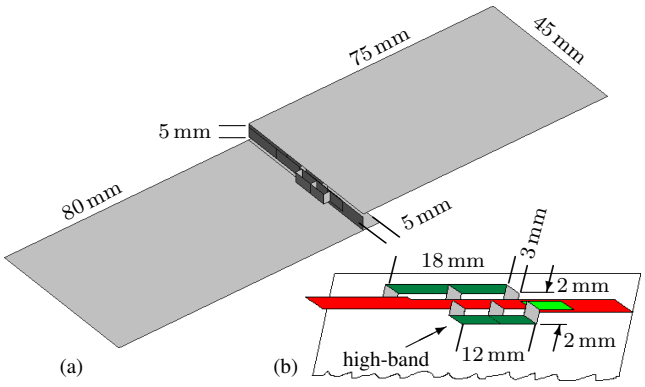

Fig. 4. Simulation model for a dual-feed, penta-band antenna concept study: (a) chassis, (b) view on S-shaped interconnection with inductive couplers, flip removed. Strips are 3 mm wide and at 2 mm distance.

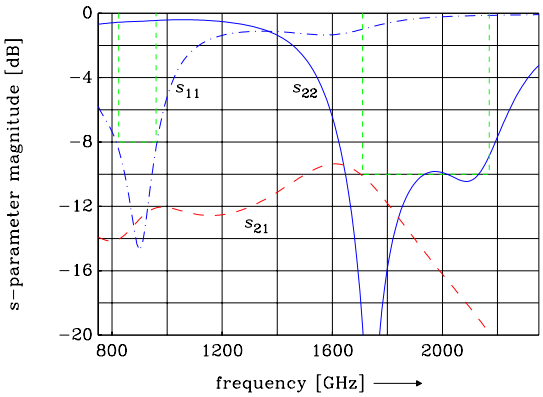

Fig. 5. Simulated scattering parameters for the dual-port antenna of Fig. 4. Port 1 and 2 are the low-band and high-band ports, respectively.

but slightly moved inwards on the base part to increase the resonance frequency of the first mode. Two parallel resonant inductive couplers are placed broadside on the base–flip interconnection, one on either side. Each coupler is a short section of strip-line parallel to the interconnection, grounded to the latter at one end and capacitively terminated at the other. A feeding tap is placed in-between. The coupler on the rear side in Fig. 4 is tuned to low-band (GSM850/900), the other to high-band (DCS/PCS/UMTS). The couplers occupy a volume of only $0.11\,\text{cm}^3$ and $0.08\,\text{cm}^3$, respectively.

Simulated scattering parameters for the dual-port design of Fig. 4 are shown in Fig. 5. s_{11} refers to the low-band port and s_{22} to the high-band port. The low-band covers the $824\ldots960\,\text{MHz}$ range with $8\,\text{dB}$ return loss. The high-band is slightly displaced from the target DCS/PCS/UMTS band ($1710\ldots2170\,\text{MHz}$) but exposes a sufficiently large $10\,\text{dB}$ bandwidth ($> 480\,\text{MHz}$). Isolation is better than $12\,\text{dB}$ in low-band and $10\,\text{dB}$ in high-band.

VI. Miniature DVB-H antenna

Digital video broadcast for handhelds (DVB-H) is currently a topic of large interest. Due to the low frequency range allocated for this service ($470\ldots702(862)\,\text{MHz}$) and its large

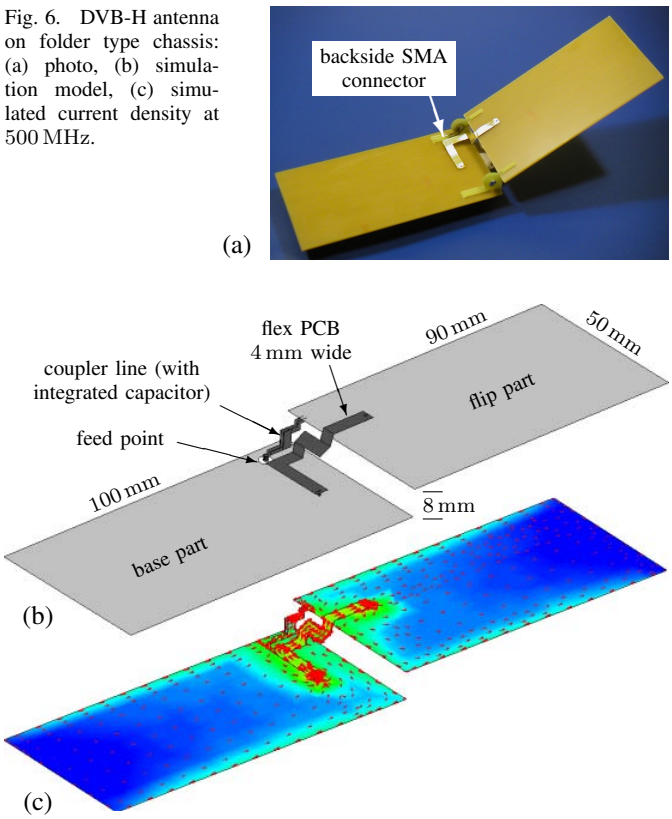

Fig. 6. DVB-H antenna on folder type chassis: (a) photo, (b) simulation model, (c) simulated current density at 500 MHz.

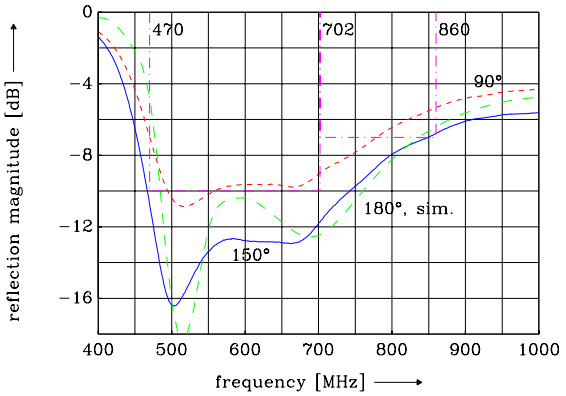

Fig. 7. Measured input reflection magnitude for DVB-H antenna of Fig. 6 at 150° (solid) and 90° (short dashes) opening angle and simulation results for 180° (long dashes).

40 % (60 %) fractional bandwidth, design of internal antennas is considered difficult. Large external flap type constructs have been used in early devices. As illustrated below for an open state folder type phone, chassis centric design and use of inductive couplers permits much more effective solutions.

A mockup photo is given in Fig. 6a and the simulation model in Fig. 6b. Base and flip part are made from single side cladded 1.5 mm FR4 boards. The interconnection between base and flip part is a flexible foil of 4 mm width and 54 mm total length with via connections to PCB ground at either end. The bare chassis exposes its first (dipole mode) resonance at 530 MHz. Realization of the DVB-H antenna is accomplished by merely adding a series resonant type inductive coupler after Figs. 3b,d. Conductor and capacitor are integrated with the hinge construction. The 2.3 pF capacitor is of rotary type, realized by two opposing ring shaped patches centered about the hinge axis. Instead an SMD capacitor could equally well be used in combination with a flexible connection. The flip part end of the line is connected to PCB ground. The base part end connects to a backside SMA connector. The extra device volume required for this "antenna" is essentially zero. Measured input reflection magnitudes at 150° (mechanical limit) and 90° opening angle between flip and base part are shown in Fig. 7. When fully open (150°) a return loss of 7 dB is observed over the full UHF band IV/V and more than 10 dB in the 470 . . . 702 MHz range. In the latter range some absorption via the external feed cable (with ferrite rings) must be accounted for. Simulation results (Fig. 7), however, confirm the viability of a free space 10 dB bandwidth of 275 MHz.

VII. Conclusion

A novel approach to the realization of wide-band mobile phone antennas with extremely small occupied extra volume, based on chassis tuning and inductive couplers has been presented and verified by simulation and measurement. Although limited to the open state of folder type, slider type and similar form factors, the excellent properties and the small volume suggest the use of this concept for dedicated open state antennas.

References

[1] P. Vainikainen, J. Ollikainen, O. Kivekäs, and I. Kelander, "Resonator-based analysis of the combination of mobile handset antenna and chassis," *IEEE Trans. Antennas Propagat.*, vol. 50, no. 10, pp. 1433–1444, Oct. 2002.

[2] J. Villanen, J. Ollikainen, O. Kivekäs, and P. Vainikainen, "Compact antenna structures for mobile handsets," in *3rd COST 284 Management Committee Meeting Workshop*, Budapest, Oct. 2003. [Online]. Available: http://www.ctsystemes.com/zeland/publi.htm

[3] R. F. Harrington and J. R. Mautz, "Theory of characteristic modes for conducting bodies," *IEEE Trans. Antennas Propagat.*, vol. 19, no. 5, pp. 622–628, Sept. 1971.

[4] M. Cabedo-Fabres, E. Antonino-Daviu, A. Valero-Nogueira, and M. Ferrando-Bataller, "On the use of characteristic modes to describe patch antenna performance," in *Proc. IEEE Antennas and Propagation Society Int. Symp. Digest*. Columbus, OH: IEEE, June 2003, pp. 712–715.

[5] E. Antonino-Daviu, M. Cabedo-Fabres, M. Ferrando-Bataller, and J. Herranz-Herruzo, "Analysis of the coupled chassis-antenna modes in mobile handsets," in *Proc. IEEE Antennas and Propagation Society Int. Symp. Digest*. Monterey: IEEE, June 2004.

[6] E. Antonino-Daviu, M. Cabedo-Fabrs, M. Ferrando-Bataller, A. Valero-Noguiera, and M. Martnez-Vazquez, "Novel antenna for mobile terminals based on the chassis-antenna coupling," in *IEEE AP-S Int. Symp. and URSI National Radio Sci. Meeting*. Washington, DC: IEEE, July 2005.

[7] W. L. Schroeder, C. Tamgue Famdie, and K. Solbach, "Utilisation and tuning of the chassis modes of a handheld terminal for the design of multiband radiation characteristics," in *IEE Conference on Wideband and Multi-band Antennas and Arrays*, Birmingham, UK, Sept. 2005.

[8] W. L. Schroeder, P. Schmitz, and C. Thome, "Miniaturization of mobile phone antennas by utilization of chassis mode resonances," in *Proc. German Microwave Conference – GeMiC 2006*, no. 7b-3, Karlsruhe, 2006.

[9] J. S. McLean, "A re-examination of the fundamental limits on the radiation Q of electrically small antennas," *IEEE Trans. Antennas Propagat.*, vol. 44, no. 5, pp. 672–676, May 1996.

射 频 和 天 线 设 计 培 训 课 程 推 荐

易迪拓培训(www.edatop.com)由数名来自于研发第一线的资深工程师发起成立，致力并专注于微波、射频、天线设计研发人才的培养；我们于 2006 年整合合并微波 EDA 网(www.mweda.com)，现已发展成为国内最大的微波射频和天线设计人才培养基地，成功推出多套微波射频以及天线设计经典培训课程和 ADS、HFSS 等专业软件使用培训课程，广受客户好评；并先后与人民邮电出版社、电子工业出版社合作出版了多本专业图书，帮助数万名工程师提升了专业技术能力。客户遍布中兴通讯、研通高频、埃威航电、国人通信等多家国内知名公司，以及台湾工业技术研究院、永业科技、全一电子等多家台湾地区企业。

易迪拓培训课程列表：http://www.edatop.com/peixun/rfe/129.html

射频工程师养成培训课程套装

该套装精选了射频专业基础培训课程、射频仿真设计培训课程和射频电路测量培训课程三个类别共 30 门视频培训课程和 3 本图书教材；旨在引领学员全面学习一个射频工程师需要熟悉、理解和掌握的专业知识和研发设计能力。通过套装的学习，能够让学员完全达到和胜任一个合格的射频工程师的要求…

课程网址：http://www.edatop.com/peixun/rfe/110.html

ADS 学习培训课程套装

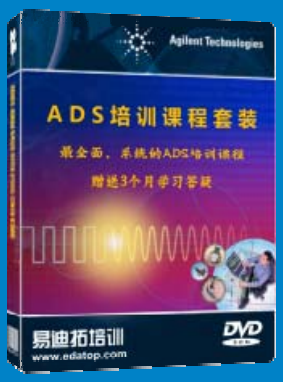

该套装是迄今国内最全面、最权威的 ADS 培训教程，共包含 10 门 ADS 学习培训课程。课程是由具有多年 ADS 使用经验的微波射频与通信系统设计领域资深专家讲解，并多结合设计实例，由浅入深、详细而又全面地讲解了 ADS 在微波射频电路设计、通信系统设计和电磁仿真设计方面的内容。能让您在最短的时间内学会使用 ADS，迅速提升个人技术能力，把 ADS 真正应用到实际研发工作中去，成为 ADS 设计专家...

课程网址： http://www.edatop.com/peixun/ads/13.html

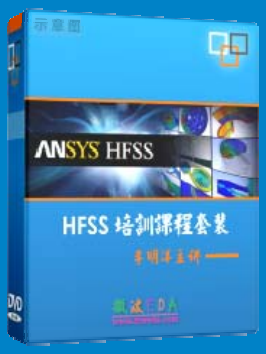

HFSS 学习培训课程套装

该套课程套装包含了本站全部 HFSS 培训课程，是迄今国内最全面、最专业的 HFSS 培训教程套装，可以帮助您从零开始，全面深入学习 HFSS 的各项功能和在多个方面的工程应用。购买套装，更可超值赠送 3 个月免费学习答疑，随时解答您学习过程中遇到的棘手问题，让您的 HFSS 学习更加轻松顺畅…

课程网址：http://www.edatop.com/peixun/hfss/11.html

CST 学习培训课程套装

该培训套装由易迪拓培训联合微波 EDA 网共同推出，是最全面、系统、专业的 CST 微波工作室培训课程套装，所有课程都由经验丰富的专家授课，视频教学，可以帮助您从零开始，全面系统地学习 CST 微波工作的各项功能及其在微波射频、天线设计等领域的设计应用。且购买该套装，还可超值赠送 3 个月免费学习答疑…

课程网址：http://www.edatop.com/peixun/cst/24.html

HFSS 天线设计培训课程套装

套装包含 6 门视频课程和 1 本图书，课程从基础讲起，内容由浅入深，理论介绍和实际操作讲解相结合，全面系统的讲解了 HFSS 天线设计的全过程。是国内最全面、最专业的 HFSS 天线设计课程，可以帮助您快速学习掌握如何使用 HFSS 设计天线，让天线设计不再难…

课程网址：http://www.edatop.com/peixun/hfss/122.html

13.56MHz NFC/RFID 线圈天线设计培训课程套装

套装包含 4 门视频培训课程，培训将 13.56MHz 线圈天线设计原理和仿真设计实践相结合，全面系统地讲解了 13.56MHz 线圈天线的工作原理、设计方法、设计考量以及使用 HFSS 和 CST 仿真分析线圈天线的具体操作，同时还介绍了 13.56MHz 线圈天线匹配电路的设计和调试。通过该套课程的学习，可以帮助您快速学习掌握 13.56MHz 线圈天线及其匹配电路的原理、设计和调试…

详情浏览：http://www.edatop.com/peixun/antenna/116.html

我们的课程优势：

※ 成立于 2004 年，10 多年丰富的行业经验，

※ 一直致力并专注于微波射频和天线设计工程师的培养，更了解该行业对人才的要求

※ 经验丰富的一线资深工程师讲授，结合实际工程案例，直观、实用、易学

联系我们：

※ 易迪拓培训官网：http://www.edatop.com

※ 微波 EDA 网：http://www.mweda.com

※ 官方淘宝店：http://shop36920890.taobao.com